Reports

Jupiter's Atmosphere: Problems and Potential of Radio Occultation

Abstract. *The atmospheric temperature-pressure profiles derived from the Pioneer 10–Pioneer 11 radio occultation experiment are mutually consistent but differ markedly from the results of other investigations. Current studies indicate that the occultation interpretation contains errors that were made very large by an inherent magnification effect, and that these errors have both geometrical and equipment sources. The apparent consistency between the Pioneer 10 and the Pioneer 11 results must be considered fortuitous. Despite these difficulties, the occultation technique, when optimally instrumented and carefully interpreted, retains its potential for atmospheric profile measurements of high accuracy and resolution.*

The Pioneer 10–Pioneer 11 radio occultation measurements of the atmosphere of Jupiter have been analyzed by Kliore *et al.* (*1*) to yield temperature-pressure (T-p) profiles markedly at odds with the results of other experiments and theory (*2*). For example, the T values at given p levels are as much as four times the expected values. A major source of error, identified by Hubbard *et al.* (*3*), has been due to the neglect of planetary oblateness in the original atmospheric analyses (*4, 5*). I have developed independently the same "sensitivity factor" used to uncover this problem and have employed it to illustrate and evaluate the magnification of possible errors due to equipment, ionospheric, and other geometrical factors. There are large errors in the original profiles that arise from a combination of sources.

The purpose of this report is to describe the apparent nature of the problems that have been encountered in the Pioneer experiment, and to indicate that the occultation technique nevertheless has the potential for detailed studies of the atmospheres of Jupiter and the other giant planets (*6*). The attainable precision and resolution are believed to be unrivaled by other techniques, short of accurate in situ measurements. However, in order for this technique to achieve its full capability, improved radio instrumentation, mission plans that augment the occultation potential, and careful attention to the analytical, data analysis, and geometrical complexities will be necessary.

It is convenient for illustration to assume that the atmosphere of Jupiter refracts radio rays between the spacecraft and Earth by the angle

$$\alpha = \alpha_0 \left(\frac{R}{a}\right)^n \qquad (1)$$

where n is a constant and R is a reference atmospheric radius of curvature approximately equal to a, the ray impact parameter. The geometrical factors are illustrated in Fig. 1. It has been shown (*7*) that Eq. 1 results from an isothermal atmosphere of scale height $H \cong R/n$ when its refractivity is less than $1/n$. This restriction, corresponding to $p < 1.5$ atm for Jupiter, is met for the regions probed in the Pioneer experiment. Such an atmosphere has a molecular concentration proportional to $\alpha H^{1/2}$ at radius $r = a$, so that atmospheric T and p are proportional to H and to $\alpha H^{3/2}$, respectively (*7*).

Let us also assume that Earth and Jupiter are stationary and that the spacecraft moves with velocity v_s in a plane normal to the direction to Earth. Let the vertical velocity v be the component of v_s that is normal to equirefractivity contours in the atmosphere, after translation through the approximate normal distance αD, as seen in the plane of the sky (Fig. 2). From Eq. 1 and Fig. 1,

$$a = R(\alpha_0/\alpha)^{H/R} \cong \alpha D + R + vt$$

so that

$$\frac{da}{dt} = D\frac{d\alpha}{dt} + v = -\frac{aH}{\alpha R}\frac{d\alpha}{dt} \qquad (2)$$

to a first order in α, assuming v is constant. Here D is the distance between the limb and the normal plane containing v_s, and time t is measured from when $a = R$. Since the radio Doppler frequency due to α is $f = \alpha v/\lambda$,

$$\frac{d\alpha}{dt} = \left(\frac{\lambda}{v}\right)\frac{df}{dt}$$

Thus the Doppler rate is given by

$$\frac{df}{dt} = -\left(\frac{\lambda D}{v^2} + \frac{H}{fv}\right)^{-1}$$

where λ is the radio wavelength and a factor $a/R \cong 1$ has been suppressed. By rearrangement,

$$\frac{\lambda f D}{vH}\left(\frac{v^2}{\lambda D\left|\frac{df}{dt}\right|} - 1\right) = 1 \qquad (3)$$

or

$$M(S-1) = 1 \qquad (4)$$

where the dimensionless magnitude factor M and the sensitivity factor S are defined by comparison.

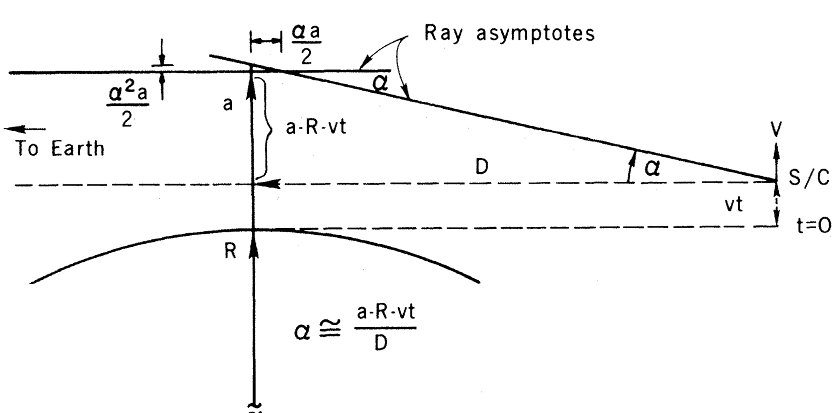

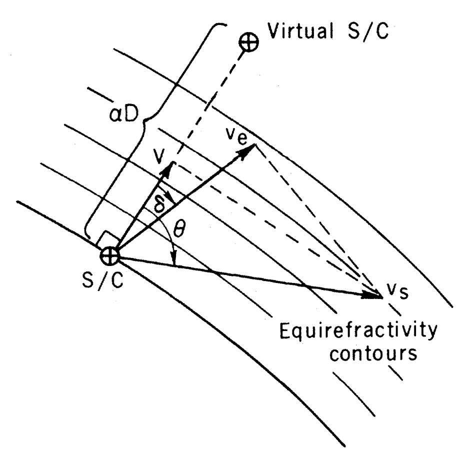

Fig. 1 (left). Simplified geometry of the occultation experiment; S/C, spacecraft. Fig. 2 (right). Spacecraft velocity components relative to atmospheric equirefractivity contours, which are assumed to lie normal to the direction of gravity.

Radio occultation experiments are based primarily on measurements of Doppler frequency as a function of time (f and df/dt) to determine scale height H as a function of height, with the use of the measured and computed geometrical factors v, D, and λ. The T-p profiles are then derived from assumed atmospheric constituents and the measured value and variations of H with height. For the atmospheres of Venus and the major planets, M in Eq. 4 may reach values of from tens to hundreds, or even thousands, when sensitive radio systems are used. Thus S only slightly exceeds unity over most of the atmospheric region probed by radio occultation. Small errors in any of the terms of S are magnified by the large M in deriving H. One can obtain a geometrical interpretation of this sensitivity by noting that S is exactly unity for ray-bending about a fixed limb ($H = 0$), as in classical knife-edge diffraction. Thus all of the information about atmospheric structure must be obtained from the small excess of S over unity.

If the measured or computed value of $|df/dt|$, D, or λ equals $(1 - \Delta)$ times its true value, or if the derived v^2 is $(1 + \Delta)$ times its true value, then the ratios of derived (false) to true values of T and p are, to a first order in Δ and for large M,

$$\frac{T_f}{T_t} \simeq 1 + M\Delta = 1 + \frac{\lambda f D}{vH}\Delta = 1 + \frac{\alpha D}{H}\Delta$$

and

$$\frac{p_f}{p_t} \simeq \left(\frac{T_f}{T_t}\right)^{3/2} \qquad (6)$$

These equations are strictly applicable only if Δ changes in such a way (proportional to M^{-1}) that the false profiles are also isothermal. However, for expository purposes, they are used here without correction (*8*).

This magnification-of-error effect does not arise when radio or optical intensity measurements are used to find atmospheric structure, since relative intensity due to refraction is approximately proportional to $(M + 1)^{-1}$. However, the intensity is also affected by absorption and scattering in the atmosphere. Even if these terms were zero, better T-p profiles can be obtained with the frequency method in radio occultation as long as S can be measured more than $M + 1$ times as accurately as intensity. This is the usual case for radio occultation so that radio intensity measurements are valuable primarily for the study of atmospheric loss mechanisms.

Four sets of Jupiter occultation measurements were made on the Pioneer 10–Pioneer 11 missions and three profiles derived (*1*). Pioneer 10 entry and exit data and Pioneer 11 entry profiles show similar but anomalously high T-p values deep in

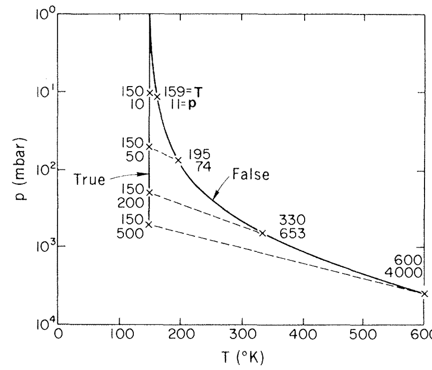

Fig. 3. True and false T-p profiles from Eqs. 5 and 6, based on the assumption that $M = 70 f/f_m$ and $\Delta = 0.043$ (*8*).

the atmosphere. Pioneer 11 exit data were reported to be unusable because of discontinuous drifts of the spacecraft oscillator frequency. The two sets of Pioneer 10 measurements also used the spacecraft oscillator, whereas the Pioneer 11 entry was made in the so-called two-way mode where the frequency reference is on Earth and the spacecraft transponder attempts to derive from the uplink signal a coherently related frequency for the downlink.

If we use the Pioneer 10 entry conditions as an example, $M \simeq 70 f/f_m$ if true H is based on a temperature of about 150°K, and f_m is the maximum value of f. Figure 3 shows true and false profiles for this M from Eqs. 5 and 6, assuming $\Delta = +0.043$ (*8*). Here maximum $T_f/T_t = 4$ where $p_f/p_t = 8$. Figure 3 is illustrative of the general character and magnitude of the relationship between the expected (true) and published (false) T-p profiles (*1*).

Of the four factors in S that could be the source of Δ, only $|df/dt|$ and v^2 are considered further (*9*). The atmospherically induced Doppler rate could be in error because of undetected frequency-generation or measurement inaccuracies, or because of other sources of ray-bending such as unmodeled effects of the ionosphere (*10*). Neglect of oblateness or uncertainties in its value can cause errors in v^2.

Since $df/dt \simeq - v^2/\lambda D \simeq -14$ hertz/sec for the Pioneer 10 entry, an undetected frequency drift of about ± 0.1 hertz/sec ($\Delta = \pm 0.007$), for example, would give a derived temperature up to 50 percent greater or less than the true value. This drift rate error is only about 4 parts in 10^{11} of the radio frequency per second, corresponding to a frequency error of 3 parts in 10^9 over the time period of this atmospheric measurement. It has been reported that the Pioneer 10 oscillator frequency changed by 3 parts in 10^6 during the Jupiter encounter (*11*), that there was a 25 percent reduction in the magnitude of the drift rate from entry to exit occultation, and that other data suggest that the rate changed in a discontinuous manner during occultation (*5*). For the Pioneer 11 exit, the correction for oblateness has now made it possible to derive T-p profiles (*3*) but significant uncertainties remain, including the effects of the spacecraft oscillator. The original Pioneer 11 entry (two-way) profile, however, moved to even higher values of T and p when oblateness was considered (*3*). It is possible in this case that the Pioneer 11 transponder could not follow the rapid uplink frequency changes but instead progressively "slipped" more cycles at a greater rate as the uplink signal became weaker and more spread in bandwidth (*12*). It is evident that error bars cannot be established for the Pioneer 10–Pioneer 11 profiles until the equipment characteristics under the signal and environmental conditions at Jupiter can be established with some confidence.

The principal effect of the oblateness of Jupiter on atmospheric profiles is the possible introduction of error in S through v^2 (*3*). In Fig. 2, v_e is the erroneous velocity component at angle δ from v, measured toward v_s. Thus

$$\Delta \simeq 2\ \delta \tan\theta \qquad (7)$$

for small δ. For the original Pioneer 10–Pioneer 11 profiles, δ is the difference between the vertical and radial (from the center of mass) directions. In the Pioneer 10 entry example, $\delta \simeq 0.05$ and $\tan\theta \simeq 1$ so that $\Delta \simeq 0.1$. Taking into account the "lag" for such a large Δ (*8*), it follows that Fig. 3 is illustrative of the size of the corrections for this example. Although the neglect of oblateness clearly represents a major error source in the initial analyses of all four occultations, this correction alone cannot reconcile the different measurements (*3*). (Uncertainty in oblateness is a further concern. For δ assumed now to result from such uncertainty and if $\delta = \pm 10^{-3}$ in this example, then there would be a $\pm$ 15 percent spread in the derived temperatures.)

The Pioneer 11 entry measurement is the only one based on two-way propagation, and the only one not improved by the oblateness correction. Although the transponder is suspect, there is also a possibility for large error in the analysis if, as in previous experiments, the measured two-way Doppler frequency were assumed to be equally divided between the uplink and the downlink. Because of the large values of v and D in the Jupiter case as compared with previous two-way experiments at Mars and Venus, aberration must be considered. The correct Doppler division is variable with height and necessitates a knowledge of the atmospheric profile for its determination, so that iterative computations must be employed. Any fixed allocation of Doppler frequency to the two paths will result in errors in T which could reach 100 percent or more.

It is not clear whether the continuing studies will make it possible to determine, from the Pioneer data, credible results of sufficient accuracy to be of significance in the study of Jupiter's atmosphere. However, certain of the problems illustrate the importance of designing spacecraft radio systems with prior consideration of their potential use in radio experiments. Important progress is being made, but much remains to be done (*13*). Continual improvements are important in related measurement, analysis, and theoretical efforts to help realize the potential of such experiments. In addition, other details can have profound effects on accuracy. For example, Eq. 7 shows that for vertical occultations or occultations near the equator or pole, oblateness uncertainties would cause only second-order errors (*14*).

It must be concluded that the apparent agreement of the published T-p profiles for Pioneer 10 and Pioneer 11 was fortuitous since they contain magnified errors due to several different sources. It is possible that appreciable uncertainty will remain after final reappraisals of the Pioneer experiment. However, the radio occultation technique has not yet reached any known fundamental limitation to its potential for accuracy and resolution in the study of any planetary atmosphere. Significant progress toward this ultimate capability is feasible for future missions (*13*).

VON R. ESHLEMAN
Center for Radar Astronomy,
Stanford University,
Stanford, California 94305

References and Notes

1. A. Kliore, G. Fjeldbo, B. L. Seidel, T. T. Sesplaukis, D. W. Sweetnam, P. M. Woiceshyn, *Science* **188**, 474 (19 A. Kliore, D. L. Cain, G. Fjeldbo, B. L. Seidel, S. I. Rasool, *ibid.* **183**, 323 (1974).
A. P. Ingersoll, G. Münch, G. Neugebauer, D. J. Diner, G. S. Orton, B. Schupler, M. Schroeder, S. C. Chase, R. D. Ruiz, L. M. Trafton, *ibid.* **188**, 472 (19 L. Wallace, M. Prather, M. J. S. Belton, *Astrophys. J.* **193**, 481 (1974).
W. B. Hubbard, D. M. Hunten, A. Kliore, *Geophys. Res. Lett.* **2**, 265 (1975).
4. Oblateness was derived from atmospheric results (*1*) but was not used in the program for obtaining these results (*3*).
5. Oblateness can also affect ionospheric profiles, but to a lesser degree. However, it was included (G. Fjeldbo, personal communication) in the derivation of these profiles; G. Fjeldbo, A. Kliore, B. Seidel, D. Sweetnam, D. Cain, *Astron. Astrophys.* **39**, 91 (1975).
6. Past occultation results for Mars and Venus are not expected to have significant errors of the type being discussed for Jupiter, primarily because of the tenuous atmosphere of Mars, the small (undetected) oblateness of Venus, the apparent equipment stability, the relatively small aberration in two-way measurements, and the correspondence of results for Venus with those from in situ measurements.
7. V. R. Eshleman, *Planet. Space Sci.* **21**, 1521 (1973).
8. For large Δ not proportional to M^{-1}, T_f and p_f should be viewed as "pulling" values, with the actual false profile "lagging" behind this pull progressively more with greater depth. The lag is due to the fact that local atmospheric temperature depends on molecular concentrations at all greater heights, so that several scale heights are needed to adjust to changes in T_f. There is a small compensating effect for very dense atmospheric regions, since M then becomes larger than the value given in Eqs. 3 and 4 whereas S stays the same. These effects do not cause a major change in the general shape of the profile, as in Fig. 3, but they do mean that that example at depth is actually representative of a Δ of approximately 10 percent. The three-halves power law relationship of Eq. 6 remains representative.
9. The values of λ and D are assumed to be known to the required precision.
10. The character and possible contribution of several ionospheric effects are included in a separate paper (V.R. Eshleman and G.L. Tyler, in preparation).
11. C. F. Hall, *Science* **183**, 301 (1974).
12. This proposed transponder behavior would produce an error of the right sign and character to help reconcile the Pioneer 11 entry profile. The transponder mode was used in this occultation because of effects of Pioneer 10 oscillator changes on measurements in the upper parts of the ionosphere.
13. In the Mariner Jupiter-Saturn missions (1977 launch), for example, radio-science should be enhanced by the use of two coherently related radio frequencies, increased transmitter powers, and radiation-hardened, ultrastable spacecraft oscillators. The transponders would not be used in occultation experiments. Additional improvements were proposed but will not be incorporated because of fiscal limitations. Certain improvements are also being incorporated in the Viking and Pioneer-Venus missions.
14. Conversely, occultations with large values of tan θ might be used to measure oblateness (with the use of mid-latitudes) or local gravity anomalies and differential rotation, if the atmospheric structure were known from probe or other occultation measurements. There is a potential experiment of this type that could be of significance in determining the reason for the apparent resonance of the rotation of Venus with the position of Earth, based on the use of the long occultations (because absorption limits α) in the Pioneer-Venus orbiter mission.
15. I thank G. L. Tyler for his many important comments on the subject of this report; T. A. Croft, G. Fjeldbo, H. T. Howard, and S. I. Rasool for additional help; and W. B. Hubbard, D. M. Hunten, and A. Kliore for a prepublication copy of their paper. This work was supported by the National Aeronautics and Space Administration.

12 May 1975

Spontaneous Fission-Neutron Fission Xenon: A New Technique for Dating Geological Events

Abstract. *A method for dating geological samples which uses fission product xenon in a manner similar to the use of radiogenic argon in the ^{40}Ar-^{39}Ar technique has been developed. The results of stepwise heating experiments for a zircon from the Ahaggar region in the Sahara are compared to the geochronology determined by the rubidium-strontium, uranium-thorium-lead, and potassium-argon dating methods.*

A notable advance in K-Ar dating consists of fast neutron irradiation of a specimen to convert some of the potassium to ^{39}Ar, and subsequent stepwise heating to release ^{39}Ar and ^{40}Ar (*1, 2*). In addition to being inherently more precise (*3*), this method has provided reliable ages even in cases of significant ^{40}Ar loss (*2*) and can directly measure disturbed ages in discordant samples (*4*). We were thus encouraged to try a similar modification of the U-Xe technique (*5*) with the aim of developing a dating method which uses the ratio of spontaneous fission xenon to neutron fission xenon to measure the age of terrestrial samples (*6*).

A zircon was chosen in an initial attempt to evaluate this technique, for two reasons. First, zircons have a relatively high uranium content and have been shown to be fairly retentive for radiogenic helium (*7*). Second, the particular zircon chosen in this study had previously been dated by the well-established U-Th-Pb method (*8, 9*). The sample, 12.1 mg of zircon M4082 ($\sim 10^3$ grains), was placed in an evacuated quartz capsule and irradiated in a thermal neutron flux for 10 hours. A 1-cm length of 1 percent Co-Al wire placed inside the quartz capsule served as a neutron flux monitor. Measurement of the γ-activity in the monitor wire relative to that in a calibrated Co-Al standard gave a value of $10.2 \pm 0.1 \times 10^{16}$ cm^{-2} for the integrated thermal neutron flux. A few days after the irradiation, the sample was transferred to a high-vacuum extraction line attached to the mass spectrometer and heated in steps of 150° from 200° to 1400°C. The gases evolved from the sample at each temperature step were exposed to Ti as it cooled from 800° to 100°C to remove the chemically reactive substances. Xenon was then separated from the remaining noble gases by adsorption on activated charcoal held at Dry Ice temperature, and its isotopic composition was measured using a high-sensitivity mass spectrometer (*10*) with sufficient resolution to separate xenon isotopes from isobaric hydrocarbons. Instrumental mass discrimination was determined by measurements of samples of xenon prepared from air and comparison with the accepted values of Nier (*11*).

From the production mechanisms it can be shown that the ratio of spontaneous fissions to neutron fissions is given by

$$\frac{S}{N} = \frac{^{238}\mathrm{U}\lambda_{sf}/\lambda_\alpha(e^{\lambda_\alpha T} - 1)}{^{235}\mathrm{U}\,\sigma_{235}\,\phi t}$$

where λ_{sf} and λ_α are the spontaneous fission and α decay constants of ^{238}U, σ_{235} is the thermal neutron fission cross section of ^{235}U, and ϕt is the integrated neutron flux. Thus, the fission xenon age for each temperature fraction in terms of measured quantities is given by

$$T = \frac{1}{\lambda_\alpha}\ln\left[1 + \left(\frac{^{235}\mathrm{U}}{^{238}\mathrm{U}}\right)\left(\frac{\lambda_\alpha}{\lambda_{sf}}\right)\left(\frac{S}{N}\right)\sigma_{235}\phi t\right]$$